Supplement of Atmos. Chem. Phys., 17, 6215–6225, 2017
http://www.atmos-chem-phys.net/17/6215/2017/
doi:10.5194/acp-17-6215-2017-supplement

Atmospheric Chemistry and Physics
Open Access

Supplement of

Technical note: Boundary layer height determination from lidar for improving air pollution episode modeling: development of new algorithm and evaluation

Ting Yang et al.

Correspondence to: Ting Yang (tingyang@mail.iap.ac.cn) and Zifa Wang (zifawang@mail.iap.ac.cn)

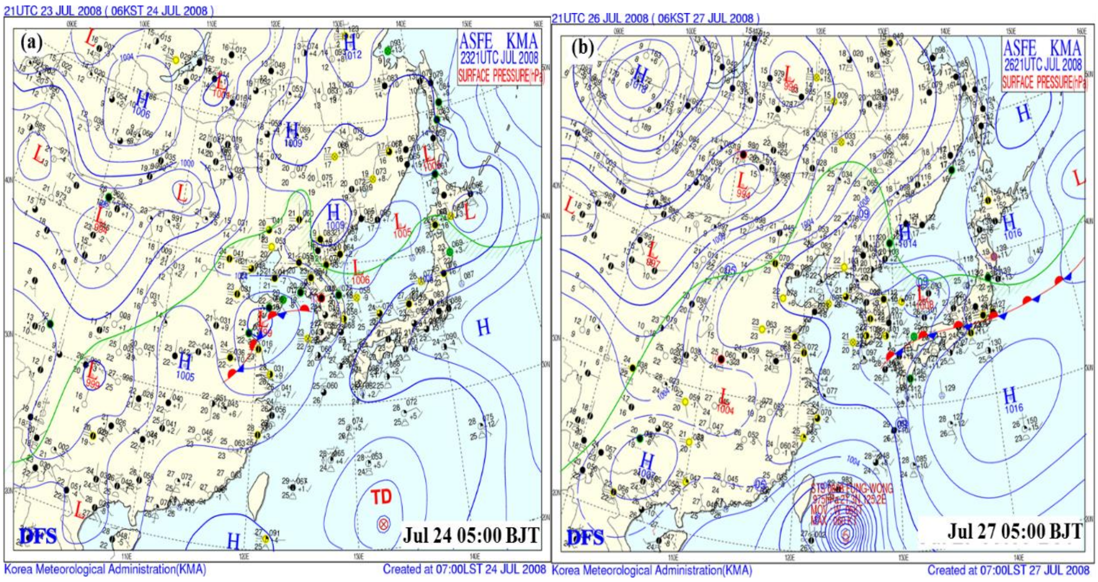

Figure S1. Surface weather maps for 05:00 am Beijing Local Time (BJT) (Source: Korea Meteorological Administration). (a) Jul.24, 2008. (b) Jul. 27, 2008.

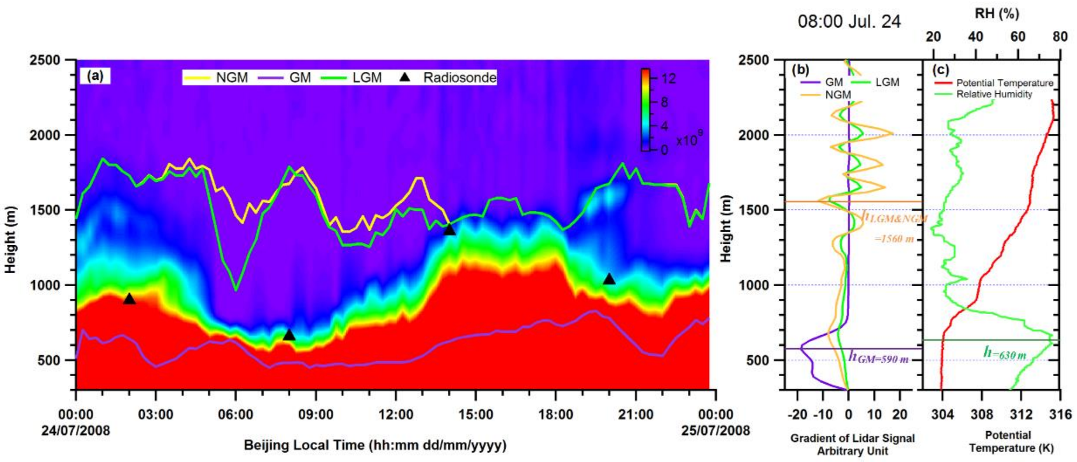

Figure S2. (a) Same as Fig. 2a but for Jul. 24; (b) Same as Fig. 2b but for 08:00 on Jul. 24; (c) Same as Fig. 2c but for 08:00 on Jul. 24.

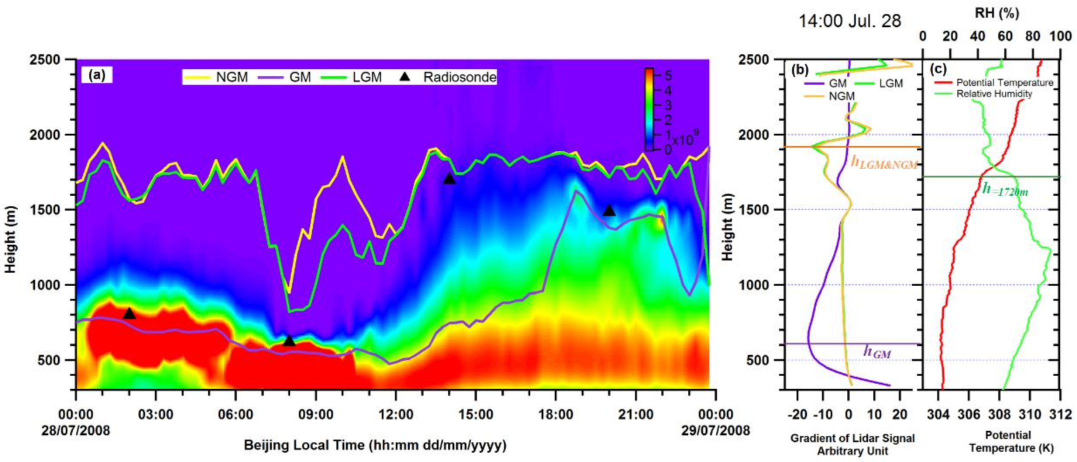

Figure S3. (a) Same as Fig. 2a but for Jul. 28; (b) Same as Fig. 2b but for 14:00 on Jul. 28; (c) Same as Fig. 2c but for 14:00 on Jul. 28.

CRGM comparison with existing ideal fit curve and wavelet methods

In ideal curve fit method, entrainment zone thickness (EZT) is set to be 2.77*s* (Steyn et al. 1999) while Haar function with a median dilation of 150 m is employed in wavelet method (Davis et al. 2000). The comparisons of the method are conducted under five typical cases including starting, undergoing, ending of a heavy polluted episode, clean atmosphere and complex multilayer boundary layer structure conditions. Detailed discussion case by case is given below.

-Undergoing heavy polluted episode (27 July)

As illustrated in Fig.S4b, at 20:00 on 27 July (heavy polluted episode), the BLH retrieved by CRGM is 1350 m, in good agreement with radiosonde result (1350 m), against 720m for ideal curve fit and a maximum of 540m for the wavelet covariance transform coefficient (Fig.S4c, d). Obviously, ideal curve fit and wavelet methods significantly underestimate the BLH by approximately 630 m and 810 m, respectively, and seem to be unable to fully capture the diurnal cycle of the BLH as showed on Fig.S4a. Such underestimate of the BLH from the wavelet method was also previously reported by several studies (Sawyer and Li, 2013; Wang et al., 2012; Su et al., 2017).

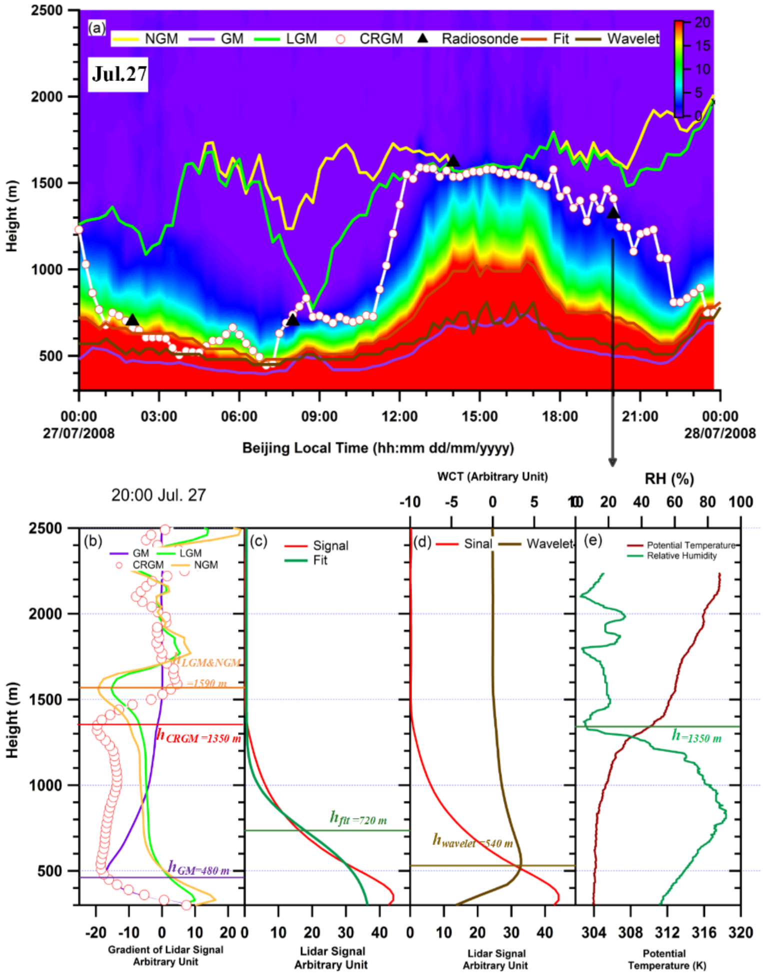

Fig.S4: (a) Evolution of the Lidar range-squared -corrected signal (RSCS) at 532 nm on 27Jul. The color bar indicates the intensity of the RSCS; the diurnal BLH retrieved by CRGM, three typical gradient method (LGM, GM and NGM), ideal curve fit and wavelet methods are illustrated as red dotted line, green, purple, yellow, origin and brown lines, respectively; (b) the profile of CRGM and the other three gradient methods and the corresponding retrieval BLH at 20:00 27 July, CRGM is illustrated in red dotted line and LGM, GM and NGM are illustrated as green, purple and yellow lines, receptively; (c) RSCS signal in red line, and ideal fit curve in green line; (d) RSCS signal in red line and wavelet covariance transform (WCT) in brown line; (e) Potential temperature and relative humidity at 20:00 on 27 July.

Starting heavy polluted episode (24 July)

The diurnal cycle of BLH retrieved by these algorithms in a starting day of heavy polluted episode and typical profiles of the methods are illustrated in Fig.S5. The results are similar with those found for undergoing polluted episode. The BLH retrievals from ideal fit curve and wavelet methods are significantly underestimation with a maximum of ~600 m and ~ 800 m, in particular in noon and afternoon.

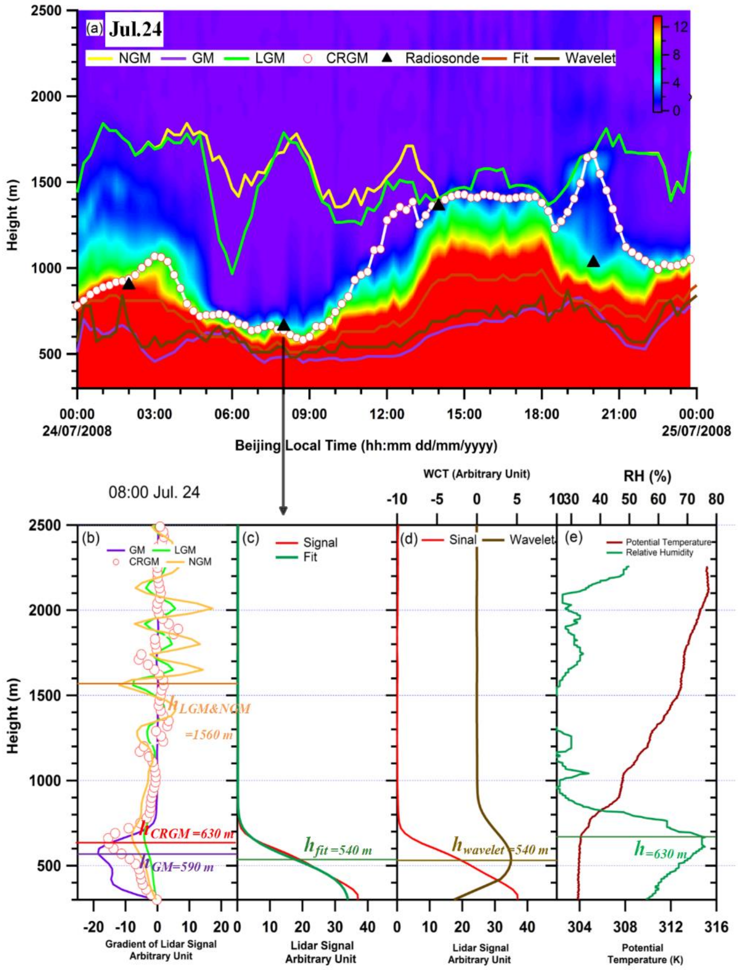

Fig.S5: same as Fig.S4, but for 24 July.

-Ending heavy polluted episode (28 July)

The comparison results are showed on Fig.S6 and confirmed persistent underestimation of BLH retrievals from the ideal fit curve and wavelet methods (with a maximum underestimation of ~700 m and ~1000 m respectively), more obvious in moon and afternoon (as found in previous cases).

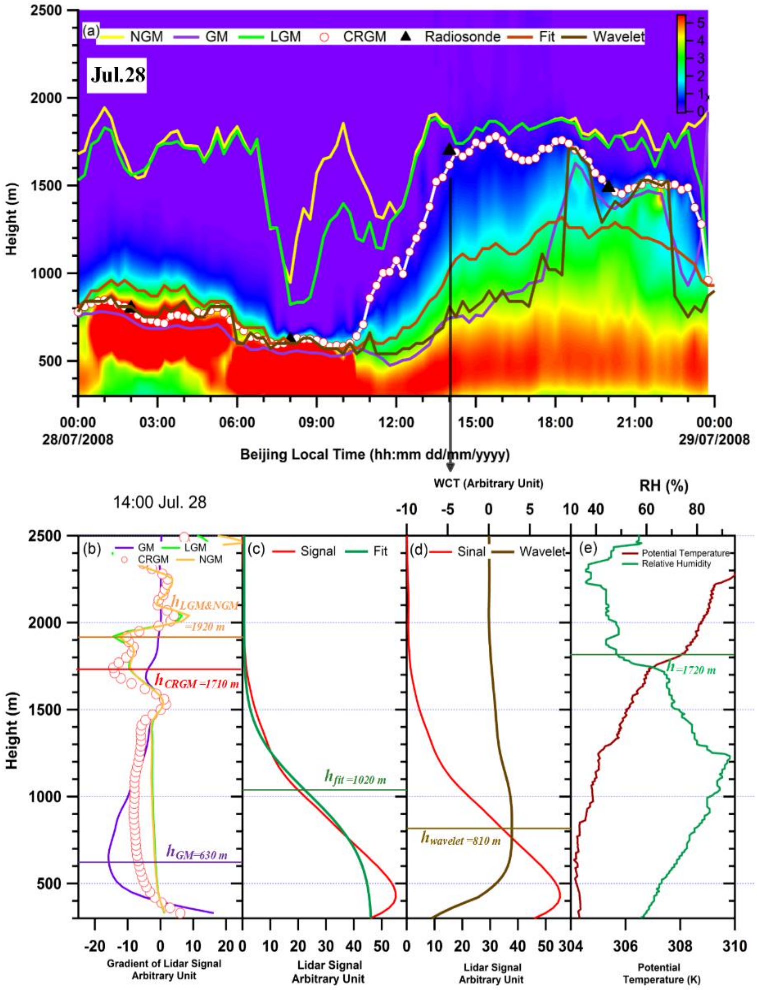

Fig.S6: same as Fig.S4, but for 28 July.

-Clean atmosphere day (9 Aug)

In this case, the results show that all retrieval algorithms capture relatively well the overall diurnal cycle of the BLH (Fig.S7). However, the retrieval from the ideal curve fit seems to present a slight underestimation of 150m at 14:00 9 Aug (Fig.S7c).

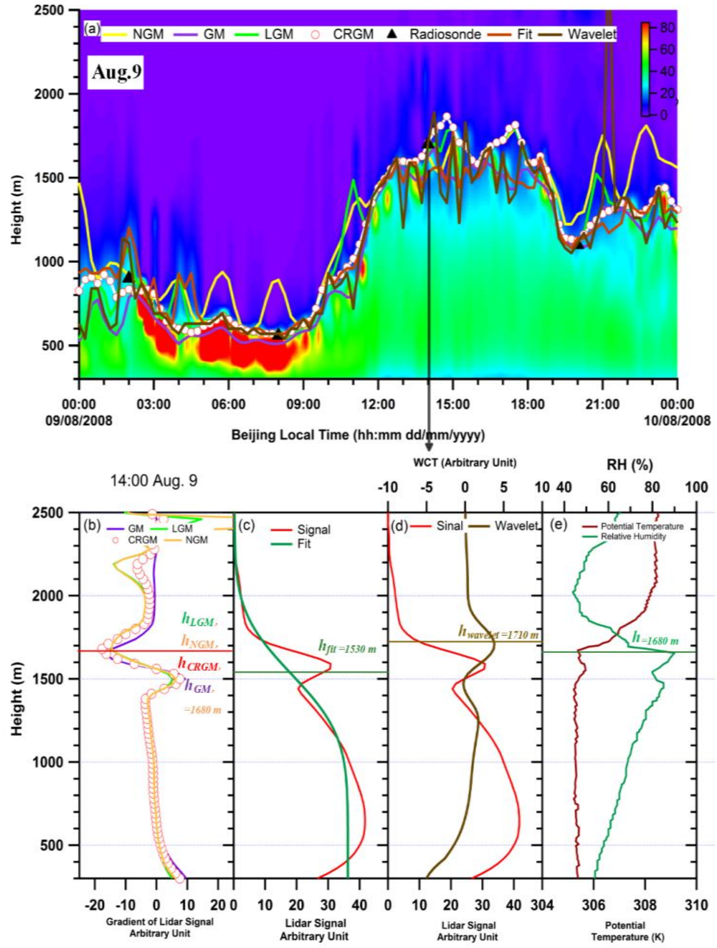

Fig.S7: same as Fig.S4, but for 9 Aug.

-Multi-layer condition

In accordance with the reviewer suggestion, we have applied all algorithms to the most complex case for multi-layer aerosol structure in our database, occurring on 26 July (Fig.S8), in order to provide further discussion on the BLH retrieval performance and limitation. Meanwhile, some improving suggestions also discussed for complex multi-layer cases.

As illustrated in Fig.S8a, an obvious two-layer aerosol structure is observed from 00:00-04:00 Jul.26, associated with a low aerosol concentration “hole” extended from ~300m to 1300m. The BLH at noon time (12:00) of the day before (Jul.25) is about 1500m, then gradually decreases to ~1300 m at 20:00 due to the ground cooling in absence of solar short-wave radiation. Significant variations of aerosol signal at upper and lower parts are also observed on 26 July between 00:00 and 04:00. Basically, the formed upper and lower parts seem not to be the natural residual and nocturnal boundary layer, but probably rather triggered by large wind driving force.

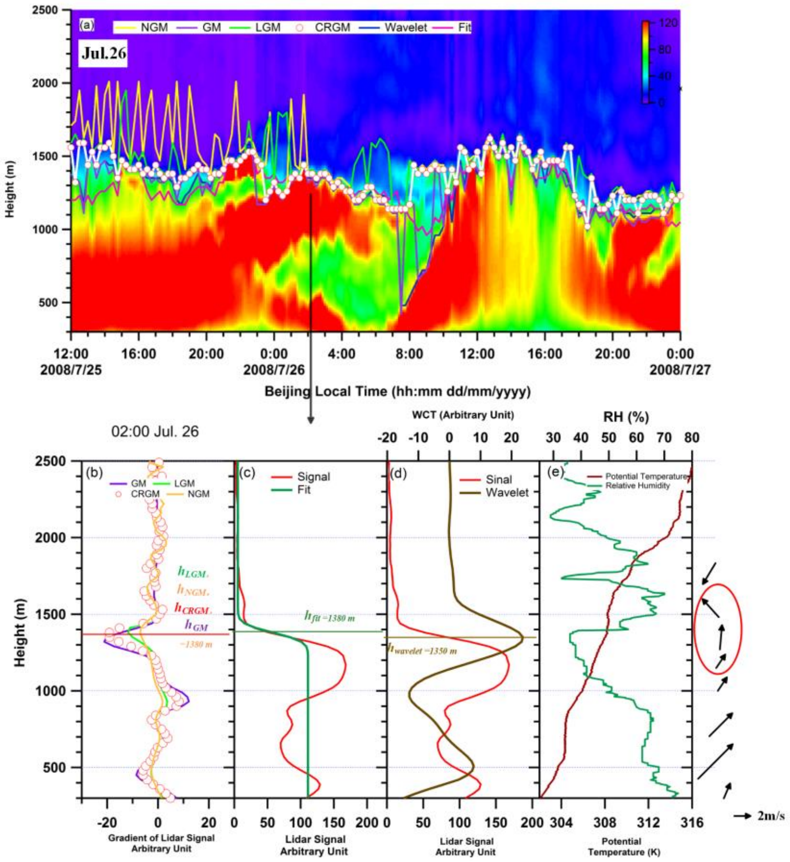

Fig.S8: same as Fig.S4, but for 26 July.

The BLH is defined at 1380m by CRGM, NGM, GM, LGM and the ideal fit curve, and at 1350 m by the wavelet transform method at 02:00 Jul.26 (Fig.S8 b, c ,d). However, all algorithms seem to only track the top of the residual layer over the multi-layer sequence (00:00-04:00 Jul. 26) and fail to capture the nocturnal layer top. Furthermore, analysis of the mean vertical profiles of the algorithms (Fig.S8b, c ,d; Fig.S9b,c,d), enables to notice two obviously negative peaks induced by CRGM, NGM, GM, LGM and the wavelet method profiles (a first largest gradient peak noticeable at ~1380 m on the top of residual layer, and a second largest peak occurring at 510 m near the top of nocturnal boundary layer). Even though all algorithms fail to track the BLH variation induced by the first largest peak, the second largest peaks work well for nocturnal boundary layer with CRGM, CRGM, NGM, GM, LGM and the wavelet method when applying the data quality control checking as described in the reply to comment (2). The retrieved nocturnal boundary layer height variation by each algorithm with data control during the multi-layer period is illustrated in Fig.S9a.

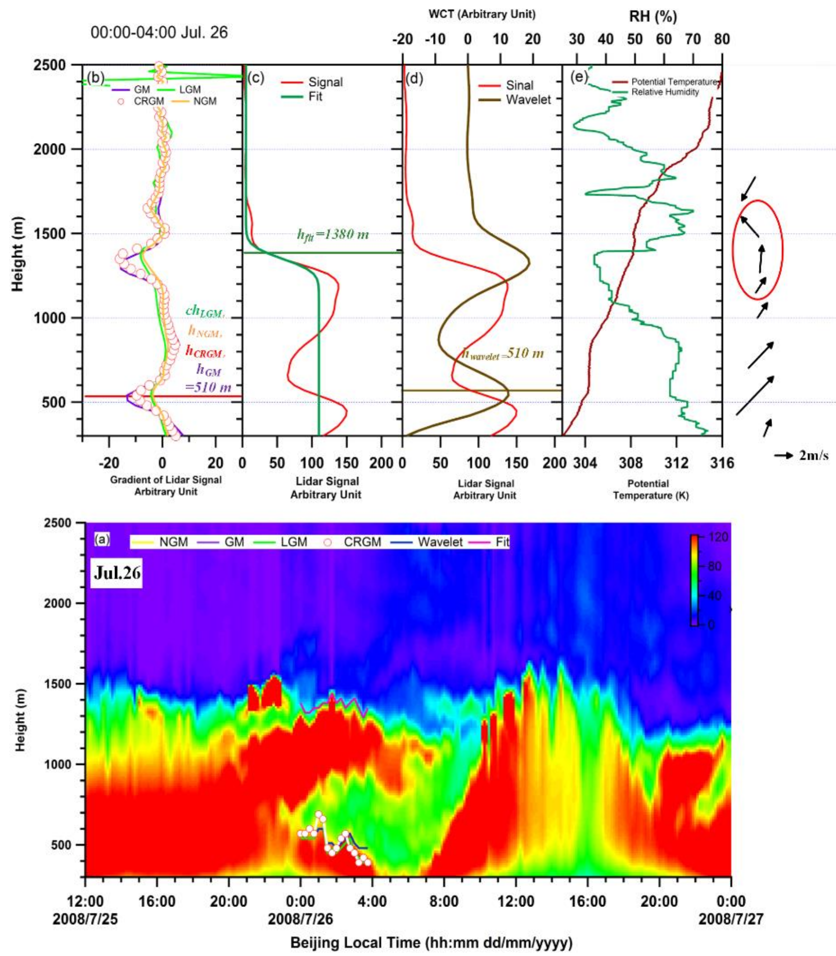

Fig.S9: same as Fig.S8, but after data quality control.